Computers and Electronics in Agriculture 110 (2015) 121–130

Contents lists available at ScienceDirect

Computers and Electronics in Agriculture

journal homepage: www.elsevier.com/locate/compag

Detecting citrus fruits and occlusion recovery under natural illumination conditions

Jun Lu [a,b], Nong Sang [a,*]

[a] Science and Technology on Multi-spectral Information Processing Laboratory, School of Automation, Huazhong University of Science and Technology, Wuhan 430074, China
[b] College of Science, Huazhong Agriculture University, Wuhan 430070, China

ARTICLE INFO

Article history:
Received 26 December 2013
Received in revised form 18 October 2014
Accepted 21 October 2014

Keywords:
Natural illumination conditions
Citrus fruits
Detection
Occlusion recovery
Partial order relation

ABSTRACT

A method based on color information and contour fragments was developed to identify citrus fruits in variable illumination conditions within tree canopy, in order to guide the robots for harvesting citrus fruits. The color properties of fruit targets within citrus-grove scene were analyzed, a preliminary segmentation method was put forward by fusing the chromatic aberration information and normalized RGB model. The set of contour fragments was constructed by detecting the significant edges of chromatic aberration map and the corners within these edges. The valid subset was chosen out by three indicators of every fragment: length, bending degree, and concavity or convexity. The combination analysis was done for these valid contour fragments, and the ellipse fitting was used for every subset of valid fragments to recover the occluded fruits. The partial order relationship was derived based on the distribution of the edge within the overlapped area. The results showed that occluded fruits were effectively recovered under natural outdoor light conditions using the proposed method, and the relative error was 5.27%. The partial order relation of fruit targets provide key cues for path planning of harvesting robot.

1. Introduction

Automated harvesting requires accurate detection and recognition of fruits within tree canopy in uncontrolled environments. Machine vision is the most important method for this task. However, occlusion, variable illumination, variable appearance and texture make this task a complex challenge.

Most works used chromatic information to differentiate fruits from background. Slaughter and Harrell (1989) and Harrell et al. (1989) distinguished citrus fruits by setting a threshold in the hue value. Ness (1989) presented an approach to solve the fruit recognition problem based on the hue difference of citrus fruit and leaves. Moct et al. (1992) presented a method to differentiate the citrus fruit from leaves based on R and G components. Xu et al. (2005) and Zhang et al. (2009) put forward a rule for segmenting citrus fruits from background based on the difference of R and B components. Wang et al. (2009) used a fusion method to get a mask to remove non-citrus background of the ratio image which was gotten by ratio transformation between R and G components. Cai et al. (2007, 2008) proposed a new method according to the self-adjusting threshold of (2R–G–B), this algorithm can recognize single or multi-fruits easily and accurately.

To sum up, most of the above methods detected citrus fruits from the tree canopy based on chromatic information. Probably the greatest difficulty arise from two aspects: one is the extreme variation of the lighting (Jimmez et al., 1999), the other is occlusion ubiquitously in natural scene.

The first difficulty lies in the extreme variation of the natural illumination. Fruits like red apples and oranges can be separated very well by color information from green backgrounds under controlled light conditions, but in an outdoor environment the changes in illumination are much greater than the chromatic difference of the fruits and the leaves. There is a technological upper limit determined by the dynamic range of the CCD of the camera. When irradiated by the sun in clear sky, part area of fruits may be saturated, with the result that the sensed image is not suitable for further processing. In this situation some patches and holes emerge in the segmentation results when using the color information and these patches cannot be removed by traditional morphologic method. When the natural illumination is very weak, such as during morning, evening, or cloud days, the integral or part surface of fruits were shaded for occlusion. These areas are so dark that their appearances have significant difference with the diffuse region in bright illumination. The shade on fruit surface cannot be detected by the traditional chromatic aberration information.

Another challenge is occlusion ubiquitously in natural scene. For self occlusion and mutual occlusion, some shades will appear

* Corresponding author.

http://dx.doi.org/10.1016/j.compag.2014.10.016
0168-1699/

on fruit surface, which will decrease the detection validity by chromatic information. On the other hand, one fruit will be divided into multiple parts for occlusion, the outer contour of fruits will not be a ideal conic.

In view of above challenges, this paper proposed a new detection method of citrus fruits within tree canopy by analyzing the salient edges of the chromatic aberration map of R and B channels in RGB color model. One reason of using chromatic aberration map of R and B channels is that it is very effectively to segment the diffuse region of fruits from orchard backgrounds (Moct et al., 1992; Xu et al., 2005; Zhang et al., 2009; Wang et al., 2009), and another important consideration is its quick calculating speed, which can meet the needs of real-time requirements.

The novel segmentation method detects the visible parts of fruits by fusing the segmentation results of chromatic aberration map and normalized RGB model. The set of contour fragments was constructed via significant edge detection and corner detection. The valid subsets were chosen out based on three indicators of every contour fragment: length, bending degree, and concavity or convexity. The combination analysis was done for these valid contour fragments, and the ellipse fitting was used to recover the fruit targets. The partial order relation was derived for all recovered fruit targets based on the distribution of edges within the overlap area.

There are three key steps in this method including preliminary segmentation, valid contour selection and occlusion recovery. The flowchart of the proposed method was shown in Fig. 1, and the details of each step were described in Section 2.

2. Materials and methods

2.1. Image acquisition

Dozens of images of citrus trees laden with fruits were obtained by Canon EOS 7D, with EF-S 18-135/3.5-5.6 IS Len during consecutive months from October to December of 2012. The brightness, contrast, shutter speed, and aperture of the camera were kept constant most of the time during imaging. These photos were obtained in an experimental citrus grove in Huazhong Agricultural University in some sunny days and some cloudy days. In sunny days, some fruits in the image were saturated for the direct sunlight. In cloudy days, many fruits were shaded by others or themselves. All the images were obtained in a stationary mode, and the resolution of them was 3456 columns by 5184 rows. They were resized to 648 × 432 pixels during the processing procedure. The CPU of the computer which was used to process and analyze the images was Intel(R) Core i7 930 2.80 GHz, the memory of which was 4 G. The operation system was Microsoft Windows XP, and the software for image processing was Matlab 7.1.

Fig. 2 is an example under natural illumination. It was found that occlusion existed ubiquitously within tree canopy, so some fruits were divided into multiple parts. The contour of fruits is not an unbroken circular or oval, but the fragments belonging to the outer contour of fruits were all smooth arc. Based on these smooth arcs, guided by the shape knowledge of fruits, the integral contour of these targets can be recovered by fitting method.

2.2. Salient edge detection

According to (Xu et al., 2005; Zhang et al., 2009), the diffuse reflection area can be detected effectively with chromatic aberration map of R and B channels. In original image with RGB color model, the value of every point is denoted as I. I is a vector, it consists of three components: R, G and B. $I = (I_{R(x,y)}, I_{G(x,y)}, I_{B(x,y)})$. The value of every point of chromatic aberration map is denoted as $I_{CAM(x,y)}$, it is calculated as follow:

$$I_{CAM(x,y)} = \begin{cases} |I_{R(x,y)} - I_{B(x,y)}| & ((I_{R(x,y)} - I_{B(x,y)}) >= 0) \\ 0 & ((I_{R(x,y)} - I_{B(x,y)}) < 0) \end{cases} \quad (1)$$

Fig. 3a is the chromatic aberration map of Fig. 2. There are significant differences between fruits and backgrounds in it, so the salient edge which surrounded the fruits was drawn from this map. Here the canny operator was chosen to detect the notable edge of fruits (Canny,1986). Three parameters should be set when using canny operator: two thresholds-upper (T_h) and lower (T_l), and the size of Gaussian filter (δ). The upper threshold set too high can miss important information. On the other hand, the lower threshold set too low will falsely identify irrelevant information (such as noise) as important. In this step, we processed more than twenty images by varying these two thresholds, and the results were judged by three group members. The more significant edges detected, the less texture details detected, the results were thought better. Based on this rule, the final thresholds were set as follow: $T_h = 0.4$, $T_l = 0.1$. δ is set to 2, it is the default value in Matlab. The salient edge could be detected preferably with these three parameters for all examples in this paper. Fig. 3b is the results of Fig. 3a with these parameters.

2.3. Constructing the set of contour fragments

In general, the contours of fruits are smooth arcs. However, the actual contours are not so ideal for occlusion by the leaves, trunks, other fruits, or the existence of highlight and shade. Some of the edges in Fig. 3b detected by canny operator belong to the outer contour of fruits, while others belong to the results of occlusion.

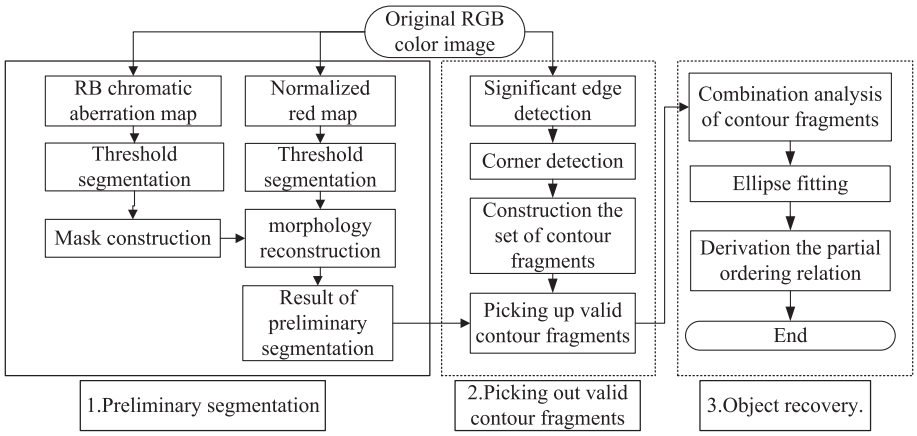

Fig. 1. Flowchart of occlusion targets recovered.

Fig. 2. An example of on-tree citrus fruits.

In order to pick out the valid outer contours of fruits, the first procedure is dividing the whole edge into continuous smooth contour fragments.

Corners in images indicate the locations where object boundaries make discontinuous changes in direction. Here corner points are significant indication of such places where occlusion exists. At first, a rotationally invariant two-phase scheme method (Teng and Hu, 1996) was used for the detection of corners, and the set of corners is denoted with Ω_C. Each individual edge was labeled with boundary tracking algorithm (Haralick and Linda, 1992), and their ends Ω_E were detected by counting the number belonging the same label within 8-neighborhood. Each end and its adjacent corner will be combined to one vertex, and the last set of vertex Ω_T was combined with Ω_C and Ω_E.

$$\Omega_T = \Omega_C \cup \Omega_E \tag{2}$$

Then, to every labeled edge, the fragment between any two adjacent vertexes was given a new label. When the traversing operation was over, the salient edge would be divided into multiple smooth contour fragments, which was denoted by a set Ω_S.

$$\Omega_S = \{\Omega_1, \Omega_2 \ldots \Omega_i \ldots \Omega_N\} \tag{3}$$

In Fig. 3c the edge between any two adjacent vertexes is a contour fragment in Ω_S. In the next section some rules will be established for choosing out the valid fragments corresponding to the outer contour of fruits.

2.4. The preliminary segmentation of the scene

In this section, the preliminary segmentation will be discussed for giving the key cues to pick out the valid contour fragments from Ω_S.

Based on the previous work in the fruit recognition problem, a great number of experiments had been done. Different color components in different color space were used, and all kinds of colors were combined to detect fruits within the tree canopy, through which more than twenty images were processed. It was found that the diffuse reflection area of fruits can be detected effectively with chromatic aberration map, and the shades on the fruit surface can be detected by normalized red map (NRM).

The chromatic aberration map (CAM) of R and B components in RGB color model was used to detect the diffuse reflection area of citrus fruits. An estimated global threshold (Gonzalez and Woods, 2003; Sonka et al., 2011) was used to segment foreground and background. Fig. 4a is the CAM of Figs. 1, and 4c is the segmentation result of Fig. 4a.

The original image with RGB color model is denoted as I. $I = (I_{R(x,y)}, I_{G(x,y)}, I_{B(x,y)})$. The value of every point of NRM is denoted as $I_{NRM(x,y)}$, it is calculated by Eq. (4). So the visible surface of fruits in every image can be detected integrally by fusing above segmentation results.

$$I_{NRM(x,y)} = I_{R(x,y)}/(I_{R(x,y)} + I_{G(x,y)} + I_{B(x,y)} \tag{4}$$

When the color space of images was transformed from RGB to NRGB (normalized RGB), the normalized R channel map (NRM) can be used to detect shade area. Fig. 4b is the NRM of Fig. 1. The segmentation result of Fig. 4b by thresholding algorithm was shown in Fig. 4d. The threshold was decided by 2D maximum between-cluster variance (Jing et al., 2001). The result showed that the shade area on fruit surface could be detected by segmentation of NRM.

The foregrounds of the segmentation results of chromatic aberration map were diffuse reflection area of fruits, which was denoted by S_{CAM}. The foreground of the segmentation results of normalized red map was dull diffuse reflection areas and shades on fruit surface, which was denoted by S_{NRM}. Fig. 4e is the result after OR operator pixel-by-pixel to the segmentation results of CAM as Fig. 4c and NAM as Fig. 4d. It was processed by morphological closing operator with a disk which has a radius of 3 pixels. The foreground of Fig. 4e is denoted as:

$$S_L = S_{CAM} | S_{NRM} \tag{5}$$

2.5. Picking out valid contour fragments

In Fig. 3c the edge between any two adjacent vertexes is a contour fragment in Ω_S. In this section some rules will be established

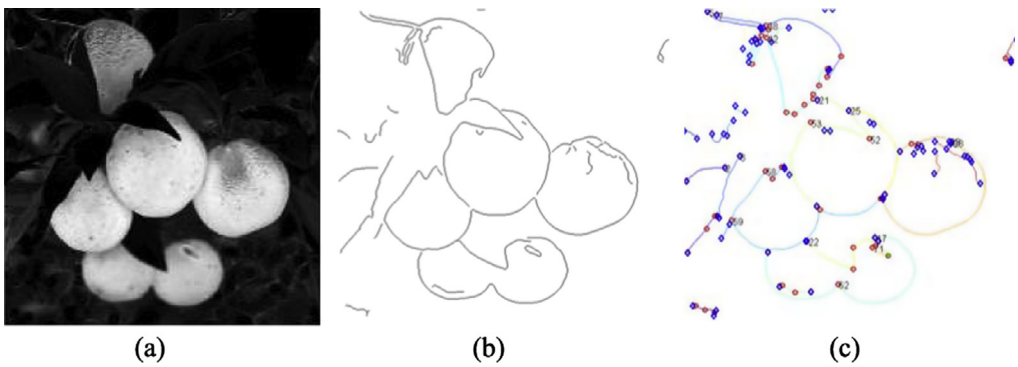

Fig. 3. Salient edge detection and corner detection: (a) the chromatic aberration map (CAM) of Fig. 1, (b) the salient edge of (a), (c) the corners (◇) and ends (○) of (b).

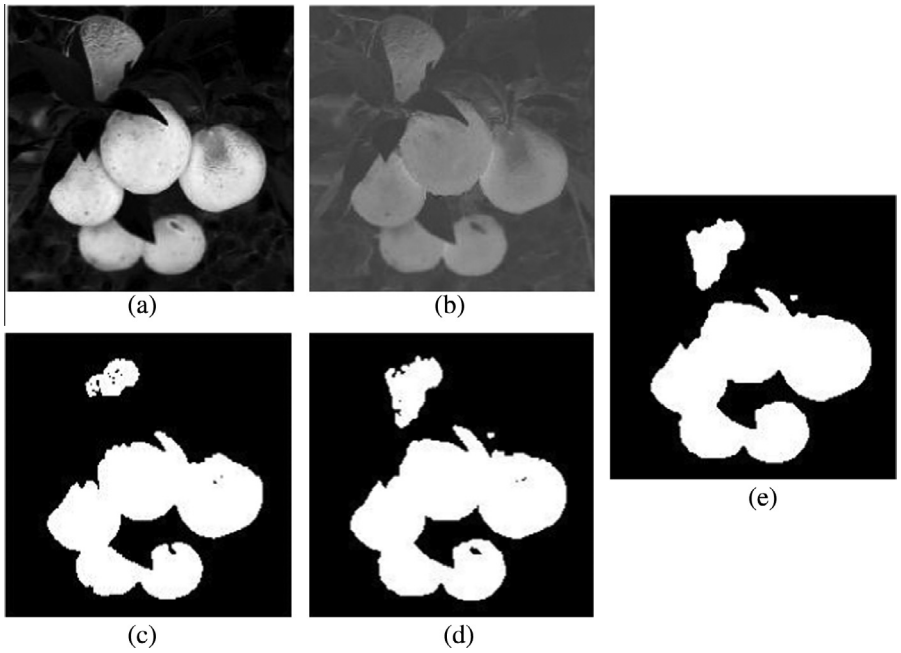

Fig. 4. Preliminary segmentation of the scene: (a) the chromatic aberration map (CAM) of Fig. 1, (b) the normalized R channel map (NRM) of Fig. 1, (c) the segmentation result of (a), (d) the segmentation result of (b), (e) the fusion result of (c) and (d).

for choosing out the valid fragments corresponding to the outer contour of fruits.

In Section 2.2, the set of contour fragments Ω_S was derived, every element Ω_i in which is a continuous smooth contour fragment. These contour fragments surrounded the fruit targets. They can be divided into two parts: one is vital contour, whose length is relatively long, and they are long straight lines or smooth curves; the other is trivial contour, whose length is very short. The trivial contours are unimportant for occlusion recovery of fruits, so they can be removed from the set Ω_S firstly. With regard to the vital contours, some of them are valid outer contour of fruits which were convex, while others were formed by occlusion, and they were concaves or long straight lines. Based on above analysis, three indicators for every contour fragment were devised as follows: length (Eq. (6)), bending degree (Eq. (7)) and concavity or convexity (Eq. (8)).

$$\begin{cases} f_1(\Omega_i) > T_1, \\ f_1(\Omega_i) = \sum_{P_i^j \in \Omega_i} 1(\Omega_i \in \Omega_s) \end{cases} \tag{6}$$

$$\begin{cases} f_2(\Omega_i) > T_2, \\ f_2(\Omega_i) = \sum_{P_i^j \in \Omega_i} d(P_i^j, l_{\Omega_i}) / \sum_{P_i^j \in \Omega_i} 1(\Omega_i \in \Omega_s) \end{cases} \tag{7}$$

$$\begin{cases} f_3(\Omega_i) > T_3, \\ f_3(\Omega_i) = \sum_{Q_i^j \in l_{\Omega_i}} \delta_{j1} / \sum_{Q_i^j \in l_{\Omega_i}} 1(\Omega_i \in \Omega_s) \end{cases} \tag{8}$$

(1) Length. It is the number of pixels of every contour fragment in the set Ω_S. The significance of this contour fragment is very low if its length $f_1(\Omega_i)$ is smaller than the threshold T_1, and it should be removed from the set Ω_S. T_1 is the lower limit which means how small the contour fragment we should take into account. If T_1 is set too large, it will miss some real contours of targets. On the contrary, if it is set too small, some false contours will be considered as real ones. For balancing of these two aspects, we did experiments on over twenty orchard scenes by varying T_1 and found that fifteen percent of the maximum length in Ω_S is an appropriate choice for T_1.

(2) Bending degree. This indicator is used to measure the flatness of every contour fragment. In Eq. (7), l_{Ω_i} is the chord connecting two ends of every contour fragment, and $d(P_i^j, l_{\Omega_i})$ is the distance between every pixel P_i^j within Ω_i and the chord l_{Ω_i}. $f_2(\Omega_i)$ is the average distance between Ω_i and its chord l_{Ω_i}, and the threshold T_2 is set to 3.0 based on many experiments.

(3) Concavity or convexity. This indicator is used for measuring whether the contour fragment is convex or concave. Q_i^j is a pixel within the chord of Ω_i. The value of δ_{j1} is 1 if Q_i^j is within the foreground of the preliminary segmentation result, and the value of δ_{j1} is 0 if not. $f_3(\Omega_i)$ is the probability that pixels within the chord of Ω_i fall into the foreground, and the threshold T_3 is set to 50% based on many experiments.

The last set of contour fragments was constructed by above three indicators from the initial set Ω_S, which was denoted by Ω_L. The valid contour fragments in Fig. 3c were shown in Fig. 5b with thick solid lines. They were denoted by a_1–a_7, and these seven contour fragments belong to six fruit targets. In the next section, the combination analysis of contour fragments will be discussed.

$$\Omega_L = \{\Omega_1, \Omega_2 \ldots \Omega_i \ldots \Omega_M\} \tag{9}$$

2.6. Combination analysis of contour fragments

In general, the unbroken contour of fruits is almost an ideal ellipse, but they are usually divided into more than one part for occlusion by leaves, trunks or other fruits. So some valid contour fragments within Ω_L probably belong to the same fruit. In Fig. 5b, the contour fragments a_2 and a_7 belong to the same fruit, so the combination analysis of contour fragments will be discussed here.

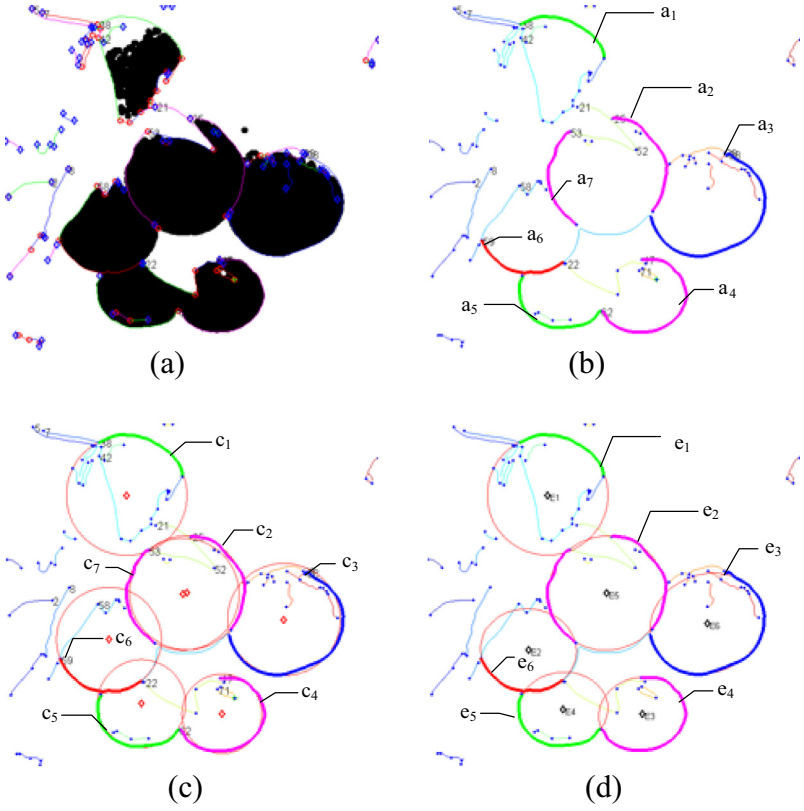

Fig. 5. The valid contour fragments and the results of occlusion recovered: (a) the edges, corners, and segmentation result, (b) the valid contour fragments (a_1–a_7), (c) the fitting circles for every fragment (c_1–c_7), and (d) the last fitting ellipses (e_1~e_6).).

Based on the fact that the shape of fruits is nearly an ellipse, and every outer contour fragment is nearly an arc. The shape knowledge of fruits was used for combination analysis of valid contour fragments.

The circle fitting based on the least squares method (Chen, 2007) was done to every valid fragment in Ω_L. The parameters of i-th circle are C_i, $C_i = \{x_{ci}, y_{ci}, r_i\}$. $\{x_{ci}, y_{ci}\}$ are coordinates of the center of C_i and r_i is its radius. Next, whether any two fragments within Ω_L can be combined together or not was judged as follow:

$$\sqrt{(x_{ci} - x_{cj})^2 + (y_{ci} - y_{cj})^2} < \min(r_i, r_j) \quad i,j \in [1, M], i \neq j \tag{10}$$

If any two circles obey the rule defined in Eq. (10), then their corresponding valid fragments Ω_i and Ω_j can be combined together. In other words, the fragments Ω_i and Ω_j belong to the same fruit, and they will be given a unified label. Table 1 shows the parameters of circles c_1–c_7, which are the fitting results of a_1–a_7. The centers of c_2 and c_7 are very close, and they obey the rule in Eq. (10). So the contour fragments a_2 and a_7 should be given a unified new label, and they belong to the same fruit.

2.7. Target fitting

To the scene with fruits in the tree canopy, every element in the set Ω_L can be regarded as a vertex of a graph, so a kind of partition was obtained for this graph based on Section 2.5, which was denoted by V in Eq. (11). Any subset in this partition corresponds to a fruit object, denoted by V_i, which was composed of valid contour fragments Ω_j–Ω_{j+k}.

$$V = \{V_1, V_2 \ldots V_i \ldots V_{N_V}\} \quad V_i = \{\Omega_j, \Omega_{j+1}, \ldots, \Omega_{j+k}\} \tag{11}$$

The pixels of V are denoted as Ψ, and the pixels in the subset V_i are denoted by Ψ_i in Eq. (12). The number of subset in V is N_V, and the number of pixels in the subset V_i is N_{V_i} .

$$\Psi = \{\Psi_1, \Psi_2 \ldots \Psi_i \ldots \Psi_{N_V}\} \quad \Psi_i = \{P_{i1}, P_{i2} \ldots P_{iN_{V_i}}\} \tag{12}$$

The ellipse fitting based on the least squares method (Chen, 2007) was done to every pixel subset Ψ_i, and the parameters of i-th ellipse are e_i. $e_i = \{x_i, y_i, A_i, B_i, \theta_i\}$. Each ellipse corresponded to a recovered contour of one fruit target. The fitting ellipses were shown in Fig. 5d, and their parameters were tabulated on Table 2.

Table 1
The circle fitting results of every contour fragment in Fig. 5c.

Label	x_c	y_c	r
c_1	111.6	186.4	92.8
c_2	262.2	279.0	88.0
c_3	303.6	428.3	86.8
c_4	449.0	332.8	61.4
c_5	433.4	209.2	68.0
c_6	334.4	159.0	80.7
c_7	264.4	273.2	86.3

Table 2
The parameters of the fitting ellipses in Fig. 5d. (x_i And y_i are the coordinates of the center of e_i. A_i and B_i are the major axis and minor axis. θ_i is the inclination of e_i).

Label	x_i	y_i	A_i	B_i	θ_i
e_1	111.6	186.4	92.8	92.8	0.00
e_2	263.0	277.0	90.4	88.1	−0.38
e_3	310.0	431.8	89.6	75.9	−0.37
e_4	449.9	331.6	66.9	56.7	−0.17
e_5	442.7	210.2	68.8	57.1	−0.05
e_6	351.1	156.9	73.8	63.6	0.11

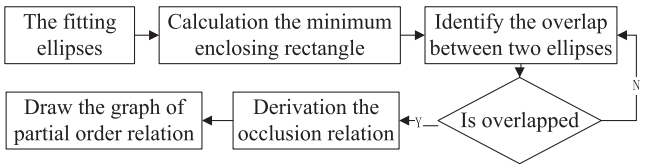

Fig. 6. The flowchart of deriving the partial order relation between fruit targets.

2.8. Deriving the partial order relation of fruit targets

Layer representation is firstly presented by Wang and Adelson for motion analysis (Adelson, 1991). Based on this idea, the concept of 2.1D sketch was then proposed firstly by (Nitzberg and Mumford, 1990; Mumford et al., 1993). In their works, T-junctions detected on region's boundaries provide the cue information of occlusion relation, and an energy function is minimized to get 2.1D sketch with experiments on some simple images. The general goal of 2.1D sketch is to resume the occluded structure part of object and find the occlusion relation (partial order) of all objects in a scene. 2.1D sketch is a very important issue in low-middle level vision tasks and remains a challenging problem yet in the literature. Solving 2.1D sketch is a critical step for scene understanding in both still images and video, such as foreground/background separation, 2.5D sketch, and motion analysis.

The concept of 2.1D sketch was used to derive the occlusion relation of the overlapped fruit targets. During the process of picking fruits automatically, it is a key problem to analyze the partial order of overlapped fruit targets, which has important significance for path planning of manipulator of picking robots.

The partial order relation was derived by the procedure in Fig. 6. At first, the minimal enclosing rectangle was calculated from the parameters of every ellipse e_i, and it is denoted by R_i. $R_i = \{x^i_{min}, x^i_{max}, y^i_{min}, y^i_{max}\}(i \in [1, N_V])$. Then the overlapped relationship between any two rectangles R_i and R_j was judged. If they overlapped, the overlapped area was denoted by R_{ij}, $R_{ij} = \{x^{ij}_{min}, x^{ij}_{max}, y^{ij}_{min}, y^{ij}_{max}\}$, and the partial order between fruit targets e_i and e_j will be discussed. The distribution of the edges within the overlapped area R_{ij} was analyzed. If the front fruit object will occlude the latter one, the edges within the overlapped area usually belong to the front fruit, and the overlapped relationship between e_i and e_j was derived based on Eq. (13).

$$f_\gamma(R_{ij}) = \alpha_\gamma \cdot D_\gamma = \alpha_\gamma \cdot \left(\sum_{P_k \in E^\gamma_{ij}} d(P_k, C_\gamma) / \sum_{P_k \in E^\gamma_{ij}} 1 \right) (\gamma \in [i,j]) \tag{13}$$

$$E^\gamma_{ij} = [P_1, P_2, \ldots, P_n] \quad (d(P_k, C_\gamma) < d_T) \tag{14}$$

$$\alpha_\gamma = 1 / \sum_{P_k \in E^\gamma_{ij}} 1 \tag{15}$$

The salient edges were detected in Section 2.1. In Eq. (13), $f_\gamma(R_{ij})$ is the product of the average distance D_γ and the weight factor α. D_γ is the average distance between the set of points E^γ_{ij} and the target $e_\gamma(\gamma = i, j)$. E^γ_{ij} are these edge points within R_{ij} that the distance between them and the target e_γ is less than the threshold d_T. Here d_T is set to 6 based on experience, and the weight factor α is set to the reciprocal of the number of edge points within E^γ_{ij}. At last the lesser the $f_\gamma(R_{ij})$ is, the closer the distance between the salient edge within R_{ij} and the target. The partial order between e_i and e_j was derived by Eq. (16). Here $e_i \Rightarrow e_j$ represent the ellipse e_i occlude the ellipse e_j.

$$\begin{cases} e_i \Rightarrow e_j & (f_i(R_{ij})\, f_j(R_{ij})) \\ e_j \Rightarrow e_i & (f_j(R_{ij})\, f_i(R_{ij})) \end{cases} \tag{16}$$

The partial order relation was derived one by one between any two fruit targets if they are overlapped. The last partial order graph of whole fruit targets in the scene can be obtained. The occlusion relation in Fig. 5d is shown in Fig. 7. The minimal enclosing rectangle of every fruit object was drawn in this figure. There are

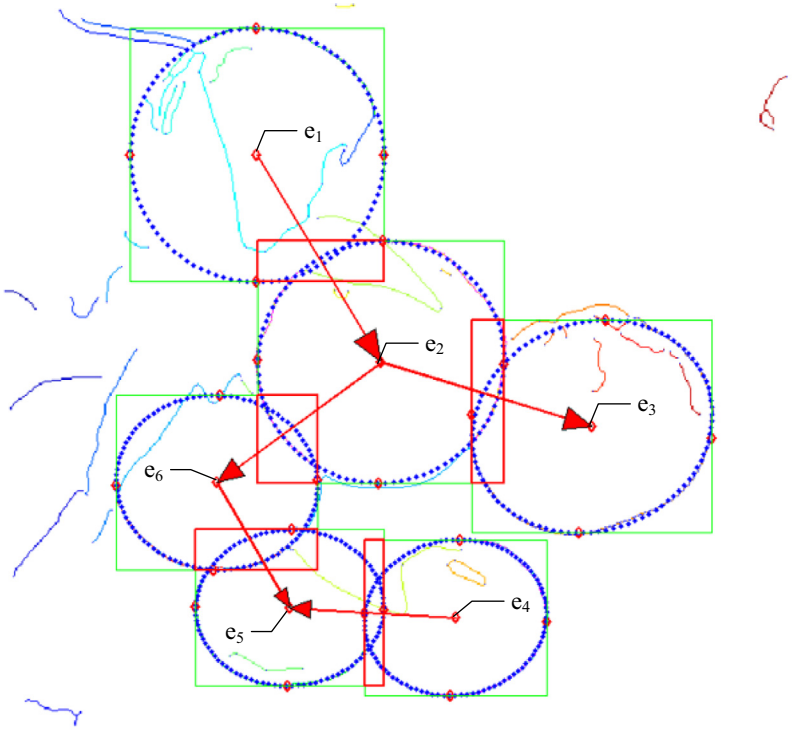

Fig. 7. The occlusion relation of fruit targets.

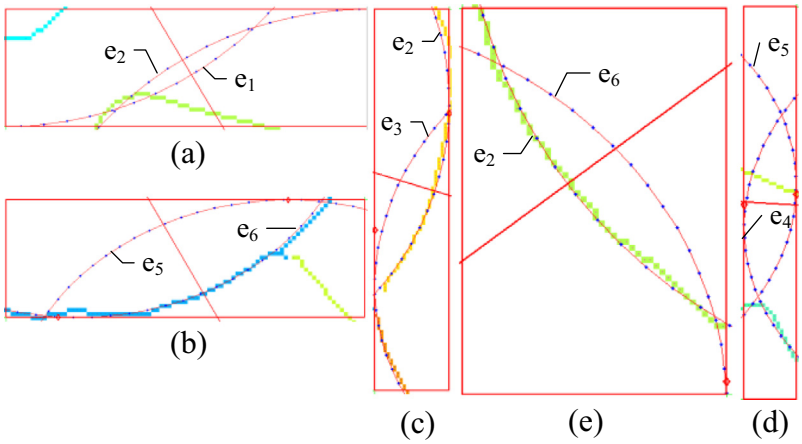

Fig. 8. The enlarging overlapped area in Fig. 7: (a) the overlap region of e_1 and e_2, (b) the overlap region of e_5 and e_6, (c) the overlap region of e_2 and e_3, (d) the overlap region of e_2 and e_6, and (e) the overlap region of e_4 and e_5.).

six fruits in Fig. 7, and five overlapped regions existed here between these fruits, which are also drawn with red rectangle in this figure. The arrow between two fruits points to the object which was occluded by another. The enlarging overlapped area was shown in Fig. 8. The edges within R_{ij} were closer with the occluding fruit targets, but farer with the occluded one. The last partial order graph of whole fruit targets was shown in Fig. 9, it is the direct cues for path planning of the manipulator of picking robot.

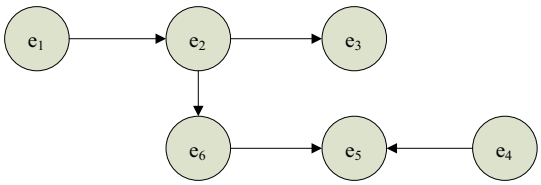

Fig. 9. The partial order graph of fruit objects in Fig. 7.

3. Results and discussions

3.1. Experimental results

Some examples are shown in Fig. 10 where the fruit targets were recovered, and the experimental results demonstrate the effectiveness of the proposed method in this paper. The original RGB images are shown in Fig. 10a. The detected salient edges and segmentation results were shown in Fig. 10b. The valid contour fragments are shown in Fig. 10c which was drawn by thick solid lines. The fitting ellipses were shown in Fig. 10d in which each ellipse corresponds to a fruit. The overlapped regions were shown in Fig. 10e by red[1] rectangles, and the occlusion relationship between overlapped fruits are also shown here. The partial order graph of whole fruits is shown in Fig. 10f.

In Fig. 10a, different degree of occlusion, shade, and highlight existed on the surface of fruit targets in these examples. Examples I–III were taken in cloudy day, most of the visible surface of fruits were diffuse region. Examples IV–VIII were taken in sunny day, in which some upper surface of fruits were saturated but lower part were shades because of self occlusion and mutual occlusion. Especially in examples VI–VIII most of fruits were occluded by others. In this paper variable illumination conditions meant that different levels of shade, highlight and diffuse region existed on the surface of fruits for varying natural illumination and occlusion.

The foreground of preliminary segmentation results in Fig. 10b are the visible parts of fruits within tree canopy. It could be found that the proposed segmentation method can detect fruits fairly complete. The last results showed that the fruit targets within tree canopy could be recovered integrally by the proposed method. The partial order relationship was derived correctly for any two overlapped fruits.

[1] For interpretation of color in Figs. 10, the reader is referred to the web version of this article.

3.2. Fitting error analysis

For quantitative measuring the proposed method, the fitting error of every recovered fruit target was calculated by the average distance between the fitting data points and their corresponding recovered ellipse. The relative error was defined by the quotient between the fitting error and the average of the major axis and minor axis of the corresponding recovered ellipse.

The fitting error was denoted by α_i and calculated by Eq. (18). The relative error was denoted by β_i and defined by Eq. (19). The sketch map for fitting error evaluation of e_i was shown in Fig. 11. P_i^j is the j-th point for fitting e_i, d_j is the lower distance between P_i^j and e_i, and α_i is the average distance between all points for fitting e_i and e_i. The parameters of the recovered fruit targets and fitting errors were shown in Table 3. The average fitting error of whole examples in Fig10 is 4.91, and the relative error is 5.27%.

$$\begin{cases} e = \{e_1, e_2 \dots e_i \dots e_{N_V}\}, \\ e_i = \{x_i, y_i, a_i, b_i, \theta_i\} \quad (i \in [1, N_V]) \end{cases} \tag{17}$$

$$\alpha_i = \sum_{P_i^j \in V_i} \inf d(P_i^j, e_i) / \sum_{P_i^j \in V_i} 1 \ (V_i \in V) \tag{18}$$

$$\beta_i = 2\alpha_i / (a_i + b_i) \quad (\Omega_i \in \Omega_a) \tag{19}$$

3.3. Time performance

For evaluating the time performance of the proposed method in this paper, the entire method was divided into three steps in Table 4.

The hardware for performance evaluation was described in Section 2.1. Table 5 listed the consuming time of every step of the proposed method. In this experiment eight images in Fig. 10 were processed. Each image was processed by 0.2193 s on average, and 36.31% of the consuming time was for image segmentation. The aim of segmentation was giving criteria to evaluate the

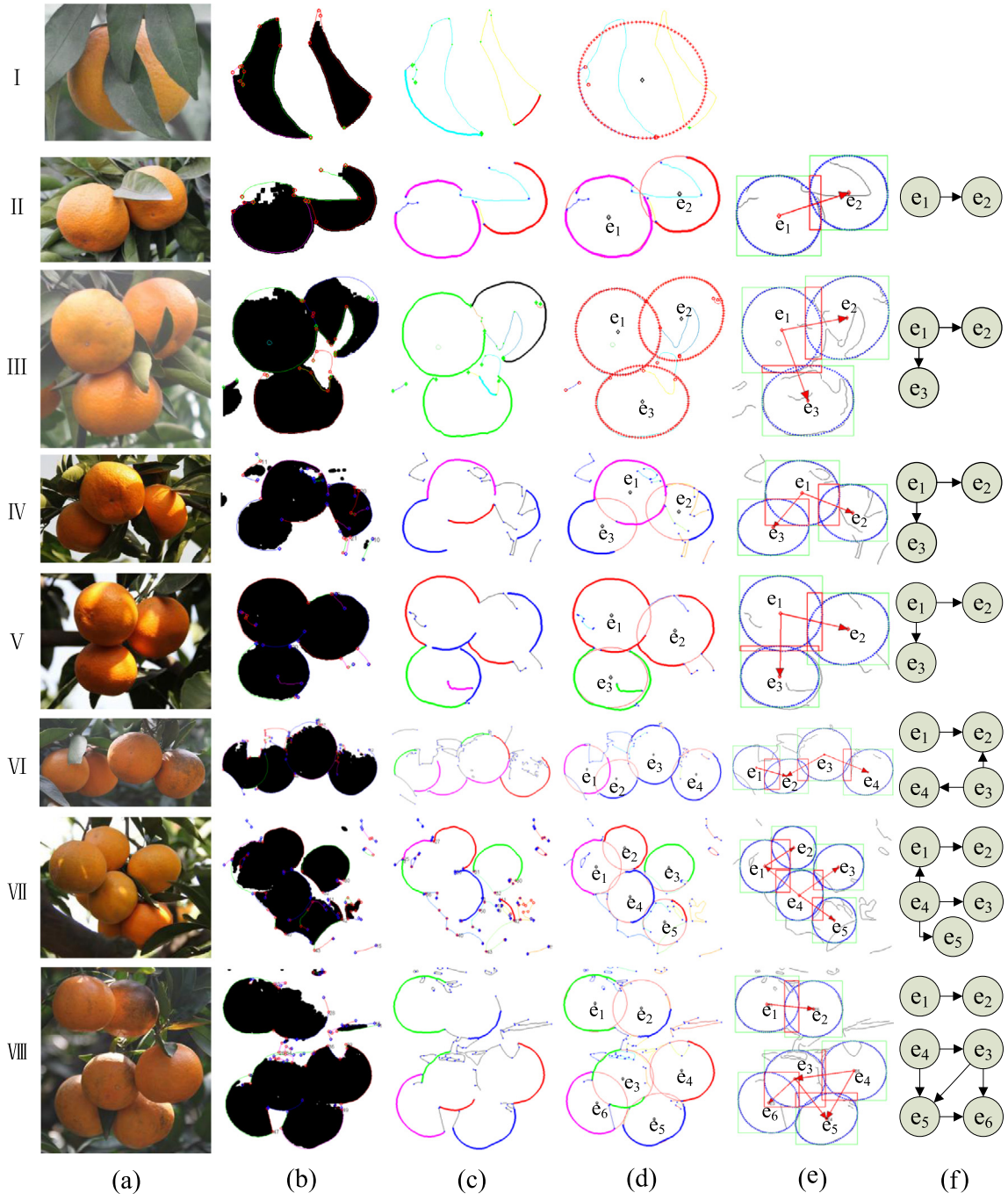

Fig. 10. The results of some examples: (a) the original RGB image, (b) the detected edges, corners and segmentation results, (c) the valid contour fragments, (d) the fitting ellipses, (e) the overlapped region and occlusion relationship and (f) the partial order graph between fruit targets.

character of concavity or convexity of each contour fragment. The gradient of contour fragments will be used as the criteria of concavity or convexity in the future work, and the step of image segmentation will be abandoned.

3.4. The analysis of threshold T_1 and T_2

In the proposed method of this paper, some problems will arise when the examples of small portions of fruit were detected. The false alarm rates will rise when the missing rates of serious hidden fruits decline.

The valid outer contours of fruits will be chosen out from the salient edge results by three criteria: from Eqs. (6)–(8). In the criterion of length in Eq. (6), the threshold T_1 will be set very small if the small contours fragments wished to be detected. But if it is set too small, some false outer contour fragments will be considered as real ones so the false alarm rates will rise. Furthermore, in the criterion of bending degree in Eq. (7), the threshold T_2 also should be set very small if the straight contour fragments wished to be detected. When it was handled like these, the contours around fruit targets which generated for occlusion will be mistaken as valid outer contours of fruits (see Tables 6 and 7).

We did two experiments to reveal the impacts of the variation of T_1 and T_2. The processed scene is the example VII in Fig. 10. In Experiment 1, T_1 is set to 0.15 and T_2 is changed. The details of

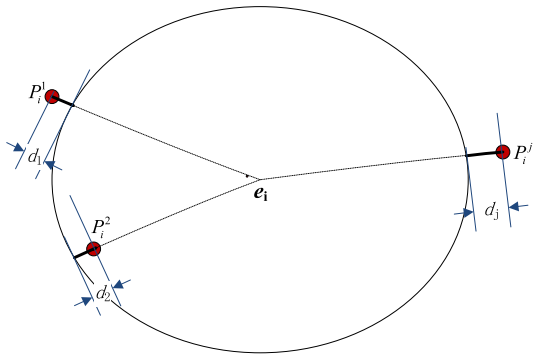

Fig. 11. The sketch map for fitting error evaluation.

detected results were shown in Table 6. In Experiment 2, T_2 is set to 3 and T_1 is changed. The results were shown in Table 7.

Here the fruits which were occluded more than 80% were thought as serious hidden ones, they were marked as SO (serious occluded). The number of serious hidden fruits (N_{SO}) in the processed scene is 3. Otherwise they were marked as OO (ordinary occluded), its number (N_{OO}) is 5 in the scene. TP is true positive samples and *FP* is false positive samples in the results. *MA* is the missing rate and *FA* is the false alarm rate. Figs. 12 and 13 showed the missing rates and false alarm rates of detection results in above two experiments. *MA* and *FA* is defined by Eqs. (20) and (21).

$$MA(i) = TP(i)/N_i \quad (i \in [SO, OO]) \tag{20}$$

$$FA = FP/\text{TOTAL} \tag{21}$$

In these two experiments, especially in Figs. 12 and Fig. 13, we can easily find that the false alarm rates will rise with the missing rates declining, however the missing rates of serious hidden fruits are also very high. Furthermore, with fruits near the picking robots were picked step by step, the serious hidden fruits will expose more and more portions. Picking fruits is a process but not a static state, so it is a good choice that the serious hidden fruits were detected gradually during the process of picking. Taking this factor into

Table 4
Three steps in the proposed method.

NO	Step description
(a)	Image segmentation
(b)	Salient edge detection, corner detection
(c)	Valid contour extraction, contour grouping, ellipse fitting

Table 5
Time performance of the proposed method.

Example (Step→)	Time span (s)			
	(a)	(b)	(c)	Sum
I	0.0783	0.0360	0.0964	0.2107
II	0.0832	0.0311	0.1223	0.2366
III	0.0916	0.0513	0.1026	0.2456
IV	0.0733	0.0353	0.0639	0.1725
V	0.0592	0.0354	0.0729	0.1675
VI	0.0869	0.0466	0.1054	0.2388
VII	0.0824	0.0335	0.1127	0.2287
VIII	0.0821	0.0514	0.1208	0.2543
Average(s)	0.0796	0.0401	0.0996	0.2193
Percentage	36.31	18.27	45.42	100.00

Table 3
The results of occlusion recovered and relative error.

Example	Ellipse	x_i	y_i	A_i	B_i	θ_i	α_i	β_i (%)
I	e_1	165.8	151.1	146.3	124.7	−0.55	6.06	4.47
II	e_1	130.1	149.7	91.3	83.2	0.49	3.33	3.82
	e_2	278.3	101.0	83.0	78.8	0.30	2.37	2.93
III	e_1	320.2	134.6	123.9	105.8	−0.79	1.47	1.28
	e_2	140.7	169.5	118.7	110.0	1.42	5.33	4.66
	e_3	212.4	365.1	126.5	96.9	−0.07	10.22	9.15
IV	e_1	205.0	107.9	93.2	88.4	0.46	2.15	2.36
	e_2	132.5	201.6	89.2	76.2	−0.23	7.87	9.51
	e_3	330.7	162.3	87.2	76.4	0.40	4.46	5.46
V	e_1	199.4	126.5	101.1	96.7	1.16	1.96	1.98
	e_2	199.0	292.6	96.1	84.0	0.21	6.94	7.70
	e_3	357.3	165.7	99.5	90.1	−0.71	1.07	1.13
VI	e_1	119.7	244.2	110.1	99.4	0.19	7.23	6.90
	e_2	260.5	283.0	105.2	76.7	−0.28	8.09	8.90
	e_3	438.8	183.6	126.2	120.0	−0.05	4.04	3.29
	e_4	643.6	264.5	118.8	101.2	−0.43	7.50	6.82
VII	e_1	107.9	156.1	83.7	82.5	−1.33	1.01	1.21
	e_2	202.1	97.0	74.0	66.8	0.39	3.15	4.47
	e_3	220.7	249.1	82.1	75.3	−0.98	1.86	2.36
	e_4	349.7	158.9	82.6	72.0	−0.27	6.28	8.12
	e_5	335.3	328.1	71.9	71.9	0.00	8.32	11.58
VIII	e_1	136.0	118.7	100.1	91.5	−0.03	5.87	6.13
	e_2	223.9	361.5	97.0	92.3	−0.27	3.08	3.25
	e_3	141.5	439.6	101.9	93.3	0.92	1.56	1.60
	e_4	323.7	491.7	101.7	78.2	−0.46	9.73	10.82
	e_5	410.8	335.5	101.6	95.9	0.25	3.19	3.23
	e_6	282.4	134.3	91.3	91.3	0.00	8.42	9.22
Avg.							4.91	5.27

Table 6
The detection results when T_1 is set to 0.15 and T_2 is changed. (TOTAL is the number of detected contour fragments. *TP* is the number of true outer contour fragments, and *FP* is the number of false ones. *TP*(SO) is the number of detected fruits which are occluded seriously, and *TP*(OO) is the number of detected examples which are not serious occluded. *MA*(SO) is the missing rates of serious occluded fruits, and *MA*(OO) is the missing rates of ordinary occluded fruits. *FA* is the false alarm rates).

NO	T_2	TOTAL	*TP*	*FP*	*TP*(SO)	*TP*(OO)	*MA*(SO)	*MA*(OO)	*FA*
1	5.00	4	4	0	0	4	1.00	0.20	0.00
2	4.50	5	5	0	0	4	1.00	0.20	0.00
3	4.00	5	5	0	0	4	1.00	0.20	0.00
4	3.50	8	7	1	0	5	1.00	0.00	0.13
5	3.00	8	7	1	0	5	1.00	0.00	0.13
6	2.50	10	8	2	0	5	1.00	0.00	0.20
7	2.00	12	8	4	0	5	1.00	0.00	0.33
8	1.50	15	10	5	1	5	0.67	0.00	0.33
9	1.00	15	10	5	1	5	0.67	0.00	0.33
10	0.50	16	10	6	1	5	0.67	0.00	0.38
11	0.10	16	10	6	1	5	0.67	0.00	0.38

Table 7
The detection results when T_2 is set to 3.0 and T_1 is changed.

NO	T_2	TOTAL	*TP*	*FP*	*TP*(SO)	*TP*(OO)	*MA*(SO)	*MA*(OO)	*FA*
1	0.50	2	2	0	0	2	1.00	0.6	0.00
2	0.45	4	4	0	0	4	1.00	0.2	0.00
3	0.40	5	5	0	0	4	1.00	0.2	0.00
4	0.35	5	5	0	0	4	1.00	0.2	0.00
5	0.30	6	6	0	0	4	1.00	0.2	0.00
6	0.25	8	7	1	0	5	1.00	0	0.13
7	0.20	8	7	1	0	5	1.00	0	0.13
8	0.15	8	7	1	0	5	1.00	0	0.13
9	0.10	9	7	2	0	5	1.00	0	0.22
10	0.05	11	8	3	1	5	0.67	0	0.27
11	0.02	12	8	4	1	5	0.67	0	0.33

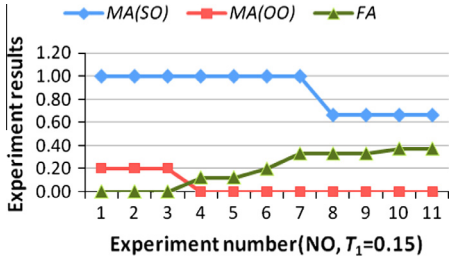

Fig. 12. The detection results when T_1 is set to 0.15 and T_2 is changed. (*MA* is missing rates and *FA* is false alarm rates).

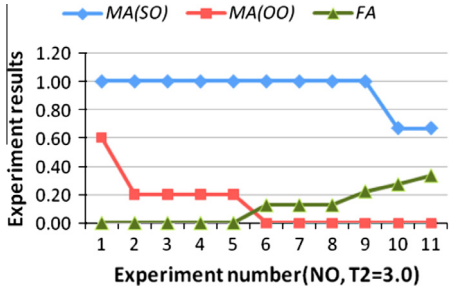

Fig. 13. The detection results when T_2 is set to 3.0 and T_1 is changed. (*MA* is missing rates and *FA* is false alarm rates).

consideration, we would rather lower the false alarm rates than detect the examples of small portions of fruits.

4. Conclusions

This paper focused on detecting citrus fruits within tree canopy under variable illumination and different degree occlusion, in order to guide the robots for harvesting citrus fruits. It applied a novel preliminary segmentation method to detect the visible parts of fruits by fusing the segmentation results of chromatic aberration map and normalized red component map. The set of contour fragments was constructed by detecting the salient edges of chromatic aberration map of R and B channels in RGB color model and the corners within these edges. The valid subsets were chosen out by three indicators of every fragment: length, bending degree and concavo–convex geometry characteristic. The combination analysis was done for these valid contour fragments, and the ellipse fitting was used for every subset of valid fragments to recover the occlusion fruit targets. The partial order relation was derived for any two overlapped targets based on the distribution of the edge within the overlapping area.

The experimental results showed that the occlusion contour was effectively recovered using the proposed method, and the relative error of occlusion recovered was 5.27%. The partial order relation of fruit targets provided the key cues for path planning of manipulator of harvesting robots.

Acknowledgements

This project was supported by NSF of China (Grant No. 31301235) and the Fundamental Research Funds for Central Universities (No. HZAU: 2013QC021).

References

Adelson, E.H., 1991. Layered representations for image coding. MIT Media Laboratory Vision and Modeling Technical Report #181, I–20.
Cai, J.R., Li, Y.L., Fang, J., 2007. Image recognition and three-dimensional location of mature oranges from nature scene. Microcomput. Inf. 23 (12), 224–225.
Cai, J.R., Zhou, X.J., Li, Y.L., 2008. Recognition of mature oranges in natural scene based on machine vision. Trans. CSAE 24 (1), 175–178 (in Chinese with English abstract).
Canny, J., 1986. A computational approach to edge detection. IEEE Trans. Pattern Anal. Mach. Intell. 8, 679–714.
Chen, J.W., 2007. The direct research of ellipse fit algorithm. Geotech. Invest. Survey. 6, 49–51.
Gonzalez, R.C., Woods, R.E., 2003. Digital Image Processing, second ed. Prentice Hall, pp. 485–486.
Haralick, R.M., Linda, G.S., 1992. Computer and Robot Vision, vol. I. Addison-Wesley, pp. 28–48.
Harrell, R.C., Slaughter, D.C., et al., 1989. A fruit-tracking system for robotic harvesting. Mach. Vision Appl. 2, 69–80.
Jimmez, A.R., Ceres, R., Pons, J.L., 1999. Automatic fruit recognition: a survey and new results using range attenuation images. Pattern Recognit. 32, 1719–1736.
Jing, X.J., Cai, A.N., Sun, J.A., 2001. Image segmentation based on 2D maximum between-cluster variance. J. China Inst. Commun. 22 (4), 71–76.
Moct, E., Pla, F., Juste, F., 1992. Vision system for the location of citrus fruit in a tree canopy. J. Agric. Eng. Res. 52 (2), 101–110.
Mumford, D., Nitzberg, M., Shiota, T., 1993. Filtering, Segmentation and Depth. In: Lecture Notes in Computer Science. Springer Press, Berlin, pp. 1–72.
Ness, Y.A., 1989. Computer Vision System for All Orange Harvesting Robot. Israel Institute of Technology, Haifa, Israel.
Nitzberg, M., Mumford, D., 1990. The 2.1D sketch. Proceedings of IEEE International Conference on Computer Vision, 138–144.
Slaughter, D.C., Harrell, R.C., 1989. Discriminating fruit for robotic harvest using color in natural outdoor scenes. Trans. ASAE 32 (2), 757–763.
Sonka, M., Hlavac, V., Boyle, R., 2011. Image Processing, Analysis, and Machine Vision, second ed. Thomson Press, pp. 487–488.
Teng, H., Hu, W.C., 1996. A rotationally invariant two-phase scheme for corner detection. Pattern Recognit. 28 (5), 819–829.
Wang, J.H., Ouyang, Q., Chen, Q.S., 2009. Adaptive recognition of different maturity citrus in natural scene. Opt. Optoelectron. Technol. 7 (5), 56–58, 62.
Xu, H.R., Ye, Z.Z., Ying, Y.B., 2005. Identification of citrus fruit in a tree canopy using color information. Trans. CSAE 21 (5), 98–101 (in Chinese with English abstract).
Zhang, Y.J., Deng, L., Li, M.Z., 2009. Estimation of citrus yield based on image processing. Trans. Chinese Soc. Agric. Mach. 40 (9), 97–99 (in Chinese with English abstract).